Acta Cryst. (1976). A**32**, 467

Measurement of the Temperature Dependence of Debye–Waller Factors by Energy-Dispersive Methods: Application to $NbC_{0.98}$

By E. F. Skelton

Naval Research Laboratory, Washington, D.C. 20375, *U.S.A.*

(*Received* 11 *August* 1975; *accepted* 12 *December* 1975)

A new method is reported for evaluating the temperature dependence of Debye–Waller factors, or equivalently the mean-square atomic displacements (MSD), from X-ray spectroscopic data. By irradiating a properly oriented single crystal with polychromatic radiation, several orders of a given Bragg reflection can be simultaneously excited at a fixed scattering angle. These multi-order peaks can then be recorded in a single measurement with an energy dispersive detector. For experiments requiring only relative intensity data, this method offers a number of improvements over conventional techniques, *e.g.*, (i) a substantial reduction in data acquisition time, (ii) a possible reduction in angular flexibility requirements and (iii) access to regions of reciprocal space which might otherwise be inaccessible. This procedure has been employed to determine the temperature dependence of the mean-square displacements of $NbC_{0.98}$ over the temperature range from 296 to 600 K. These results are compared with published values computed from a double-shell lattice-dynamical force model; the agreement is found to be satisfactory. The data have also been used to evaluate the thermal expansivity of $NbC_{0.98}$ over the temperature range of measurement; excellent agreement is found upon comparison with published thermal expansion data.

Introduction

An inherent advantage realized by the usual photographic methods of detecting X-radiation over conventional electronic techniques is the capability of simultaneously recording intensity data from a comparatively large spatial region. On the other hand, a single intensity measurement made with an electronic counter provides digital data suitable for immediate analyses in terms of crystalline structure, thermal motion, structural disorder, *etc.*, albeit from a limited region of reciprocal space. Modern energy-sensitive solid-state detectors, however, offer digital intensity data, coverage of comparatively large regions of reciprocal space and relative rapidity, all in a single measurement.

The concept of obtaining structural information with X-ray energy-dispersive techniques was originally introduced by Giessen & Gordon (1968) who noted that powder diffractometry could be pursued in much the same way as neutron time-of-flight studies. Generally speaking, X-ray data can be gathered more rapidly with energy-dispersive techniques as compared with more conventional methods: indeed, since X-ray energy measurements involve polychromatic radiation, attenuation with either filters or so-called monochromating crystals is unnecessary. However it is usually found that more accurate unit-cell parameters can still be obtained *via* conventional measurements. For example, careful lattice parameter measurements are often accurate to within 0·0001 Å, whereas Sparks & Gedcke (1972) estimate the standard deviation of their energy-dispersive lattice parameter measurements to be less than ±0·001 Å. Also, it is generally found that energy-dispersive intensity measurements are more difficult to interpret than so-called monochromatic measurements – three primary reasons being (i) the non-uniform energy spectrum of the incident radiation, (ii) the non-linear response of the detection system and (iii) the variable penetration depth in the sample. For these reasons perhaps, applications of energy-dispersive X-ray diffraction techniques have been limited largely to special environmental chambers where overall intensities or diffraction geometry might otherwise be a problem, *e.g.* at high and/or low temperatures and/or high pressures, *cf.* Freud & LaMori (1969), Albritton & Margrave (1972) and Skelton (1972).

Very recently some consideration has been given to the application of energy-dispersive X-ray diffraction measurements to single-crystal studies: Buras, Olsen, Gerward, Selsmark & Anderson (1975) have used a Si(Li) detector to perform integrated intensity measurements on highly perfect Ge single crystals. Although they obtain very good agreement between their measured and calculated intensities for the *hhh* reflections of Ge and an *R* of less than 3%, they, like other researchers, conclude that spectroscopic measurements are still somwhat inferior to more conventional techniques and the greatest utilization of such systems may lie in those areas where structural studies must be pursued under constrained conditions as noted above.

In this paper, X-ray spectroscopic techniques are used to measure simultaneously multiple Bragg reflections as a function of temperature with the purpose of determining the temperature dependence of the Debye–Waller factors of the crystal. In this application, only relative intensity data are required over comparatively small energy regions; thus many of the difficulties encountered with absolute intensity measurements or measurements spanning a large energy region are effectively avoided, while the aforementioned advantages are retained.

The evaluation of the temperature dependence of Debye–Waller factors generally requires intensity measurements of a number of independent Bragg reflections over the thermal range of interest. Such data are usually collected by fixing the temperature and then systematically measuring the reflections of interest, *cf.* Skelton & Katz (1968*a*) and Skelton, Radoff, Bolsaitis & Verbalis (1972). However, with X-ray energy-dispersive methods multiple orders of reflection from the same set of planes can be recorded simultaneously under conditions of constant scattering geometry. This new technique is applied here to determine the temperature dependencies of the Debye–Waller factors in $NbC_{0.98}$. The results are compared with recent force-model calculations.

Theory

As stated above, the objective of this work is to demonstrate how the temperature dependence of the Debye–Waller factors can be determined by means of energy-dispersive methods. Basically the information of interest is contained in the temperature dependence of the intensities of the Bragg reflections. The integrated intensity from an extended face of a mosaic crystal can be expressed as follows:

$$\varrho'(T)=CP(\theta)\Omega(E)|F_{hkl}(T)|^2, \qquad (1)$$

where C is a constant; $P(\theta)$ is a known function of the Bragg diffraction angle, θ; $\Omega(E)$ is a function of the photon energy, E; and $F_{hkl}(T)$ is the modulus of the structure factor. The function $\Omega(E)$ depends on E through a number of terms, *viz.* the energy distribution of the incident beam, the spectral response of the detection system and the absorption and fluorescence properties of the sample, quantities which, in general, may not be known.

The temperature dependence of the structure factor is related to the thermal vibrations of the crystalline lattice. The structure factor for the commonly known rock-salt lattice (space group: *Fm*3*m*), in which NbC crystallizes, can be written, within the quasi-harmonic approximation, as follows:

$$F_{hkl}(T)=\{f_{\rm Nb}\exp[-x\langle u^2_{\rm Nb}(T)\rangle] + \delta_{hkl}f_{\rm C}\exp[-x\langle u^2_{\rm C}(T)\rangle]\}\,, \qquad (2)$$

where

$$x=8(\pi\sin\theta/\lambda)^2=8(E\sin\theta)^2/2\hbar c\,, \qquad (3)$$

and

$$\delta_{hkl}=\begin{cases}+1 \text{ for } (h,k,l) \text{ all even}\\ -1 \text{ for } (h,k,l) \text{ all odd}\,.\end{cases} \qquad (4)$$

Here E is the photon energy, $\hbar$, c, λ and f have their usual meaning, and F_{hkl} is essentially zero for all mixed indices, (h,k,l). The exponential terms in equation (2) are commonly referred to as the Debye–Waller factors. Blackman (1956) has discussed the application of the classic Debye–Waller theory of thermal vibrations to a crystalline lattice of any symmetry, containing any number of atoms in the unit cell.

In the Debye–Waller theory, the MSD can be expressed in terms of a Debye temperature, $\Theta^M(T)$, through a weighted average over the lattice frequency spectrum. The appropriate expressions for a diatomic cubic lattice, such as NbC, as given elsewhere, *e.g.* Skelton *et al.* (1972), may be used here with an appropriate change in subscripts.

If two intensity measurements are considered, one performed at an arbitrary reference temperature, T_0, and the other at a different temperature, T, then the ratio of the intensities can be written as follows:

$$\frac{\varrho'(T)}{\varrho'(T_0)}=\left[\frac{P(\theta)\Omega(E)|f_{\rm Nb}\exp[-x\langle u^2_{\rm Nb}(T)\rangle]+\delta_{hkl}f_{\rm C}\exp[-x\langle u^2_{\rm C}(T)\rangle]|^2}{P(\theta_0)\Omega(E_0)|f_{\rm Nb}\exp[-x\langle u^2_{\rm Nb}(T_0)\rangle]+\delta_{hkl}f_{\rm C}\exp[-x\langle u^2_{\rm C}(T_0)\rangle]|^2}\right]. \qquad (5)$$

If the values of the MSD are known at T_0, then, in principle, a measurement of the intensity ratio at T of any two reflections, one even and one odd, will allow unique determination of $\langle u^2_{\rm Nb}(T)\rangle$ and $\langle u^2_{\rm C}(T)\rangle$.

On the left-hand side of Fig. 1, the usual relationship is depicted between the reciprocal lattice and the Ewald sphere of reflection which is drawn with a radius of $1/\lambda$. The diagram on the right-hand side of Fig. 1 schematically depicts the situation when polychromatic

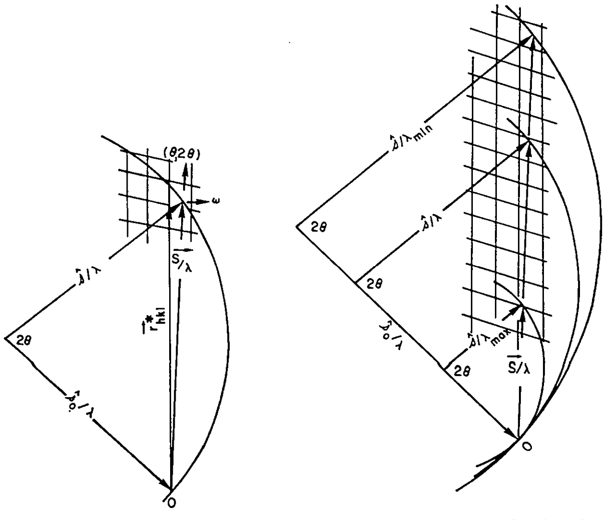

Fig. 1. Left side: Section through the Ewald sphere of reflection depicting the conventional relations between the incident and scattered beam unit vectors, $\hat{s}_0$ and $\hat{s}$, respectively, the diffraction vector $\bar{\mathbf{S}}$, and the reciprocal lattice vector $\mathbf{r}^*_{hkl}$. Right side: Schematic representation of the interaction between reciprocal lattice and the continuum of Ewald spheres encountered with polychromatic radiation.

radiation is employed. In this case, a continuum of Ewald spheres is considered, the largest being associated with the energy of the most energetic photon in the incident beam and the smallest being determined by the low-energy cut-off of the detection system. Similarly, a continuum of diffraction vectors is present ranging from $(\bar{\mathbf{S}}/\lambda_{\max})$ to $(\bar{\mathbf{S}}/\lambda_{\min})$. Thus when a reciprocal lattice vector, $\bar{\mathbf{r}}^*_{hkl}$, is coincident with $\bar{\mathbf{S}}$, then all orders of that reflection, for which $\bar{\mathbf{S}}/\lambda_{\max} \le \bar{\mathbf{r}}^*_{hkl} \le \bar{\mathbf{S}}/\lambda_{\min}$ will be simultaneously excited. (It is clear from Fig. 1 that the usual $(\theta,2\theta)$ motion will serve to shift the wavelength, or equivalently the energy, at which the various reflections are excited.) If the radiation scattered in the $\hat{s}$ direction is measured with an energy-sensitive detector spanning the energy range of interest, then all the excited reflections can be recorded simultaneously. An example is shown in Fig. 2 for a $\mathrm{NbC}_{0.98}$ crystal oriented so that $\bar{\mathbf{r}}^*_{hhh}$ is coincident with $\bar{\mathbf{S}}$; the peaks with $h=3,4,\ldots,17$ were simultaneously recorded at 296K.

Experimental procedures

All measurements were carried out on a NbC single crystal in the form of a right circular cylinder of about 6 mm diameter, chemically characterized as being $\mathrm{NbC}_{0.98}$, and supplied by Dr H. G. Smith of Oak Ridge National Laboratory. The crystal was cut so that an end face was parallel to (100) planes. The sample was mounted in a four-circle goniometer which, in turn, was mounted on a Picker biplanar diffractometer.

The sample was irradiated with X-rays from a Mo tube operated at 48 kV and 14 ma. Both conventional quasi-monochromatic and polychromatic data were collected. Initially both the incident and scattered radiation were filtered through Zr foils; the scattered radiation was measured with a NaI(Tl) detector employing standard electronic pulse-height discrimination. The beam filters were removed for the polychromatic measurements and an Ortec Si(Li) detector (7000 Series) was used to measure the scattered radiation. The Si(Li) detector output was processed through an Ortec-716 amplifier, a Nuclear-Data 180-Series analogue-to-digital converter, and analyzed with a Nuclear-Data 512-channel memory unit.

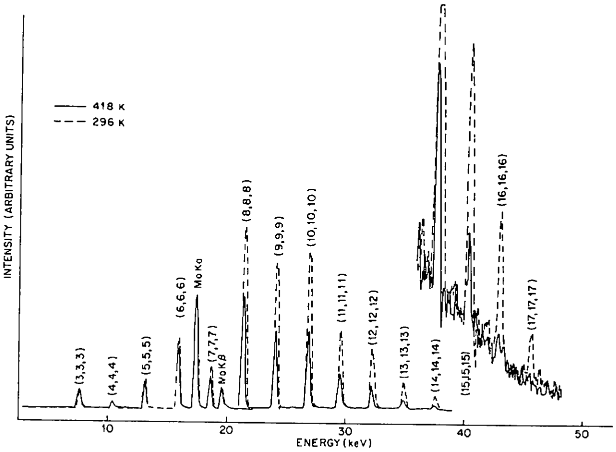

Fig. 2. Bragg energy spectra of the *hhh* reflections of $\mathrm{NbC}_{0.98}$ recorded at 296 K (dashed curve) and 418 K (solid curve). Three different amplification factors are used in plotting the data.

Energy calibration was accomplished with the use of several radioactive isotopes in addition to the Mo *Kα* and Mo *Kβ* lines present in the incident radiation. The energy resolution of the detection system was measured to be 176 ± 6 eV, based on the 5·894 keV Mn *Kα* line obtained from the decay of an Fe^{55} source with activity in the low microcurie range.

The sample temperature was continuously monitored throughout the experiment. The uncertainty in the measurement and control of the temperature is estimated to be well within ± 1 % over the thermal range involved, 296–600 K.

Prior to the energy-dispersive measurements, the integrated intensities of 95 Bragg peaks were measured at 296 K in the usual manner, *cf.* Skelton, Lin & Rothberg (1974). The crystal was then positioned so that the 777 reflection would be excited by the Mo $K\alpha_1$ line $(2\theta = 148{\cdot}29°)$, and, by rotating around the diffraction vector, the crystal orientation was checked to ensure that Renninger relections were not present at the position of measurement. The intensity of the 777 peak was measured as a function of temperature by integrating in $(\theta,2\theta)$ at a speed of $\frac{1}{16}°\ \mathrm{min}^{-1}$ from 1° below the $K\alpha_1$ peak to 1° above the $K\alpha_2$ peak; at this angle, the Mo *Kα* doublet is separated by 2·53° in 2θ. Because of the thermal expansion of the crystal, the center of the $K\alpha_1$ peak was redetermined at each temperature.

The Zr filters were then removed and the NaI(Tl) detector was replaced by the Si(Li) detecting system. With the 2θ angle left at 148·29°, the excessive Mo *Kα* radiation scattered from the (777) planes caused an extremely high counting rate with a consequent substantial increase in the dead-time of the detection system. To avoid this problem, the 2θ angle was reduced to 142·50°; at this setting the excitation energy for the 777 reflection was midway between the Mo *Kα* line (17·443 keV) and the Mo *Kβ* line (19·607 keV).

The low-energy cut-off of the detection system was set at about 6 keV and, as noted above, the X-ray tube was operated at 48 kV. Thus the 333, 444, . . . , 17,17,17 reflections were all simultaneously excited and measured (Fig. 2). Note that utilization of the energy continuum above the characteristic lines substantially increases the amount of reciprocal space which can be examined; indeed, in this instance, the highest-order *hhh* reflections observable with the Mo *Kα* and Mo *Kβ* radiation are only the 777 and 888, respectively. These higher-order reflections are especially important in this work since we are interested in the temperature dependence of the Bragg intensities and, as seen in equation

(3), the coefficient of the Debye–Waller factor varies as the square of the energy. This effect is also seen in Fig. 2, *i.e.* two spectra are plotted in the figure, one recorded at 296K (dashed curve) and the other recorded at 416K (solid curve). Note that the intensity and position of the Mo $K\alpha$ and $K\beta$ lines are thermally invariant and, as expected, the effect of temperature on the Bragg peaks increases significantly with the excitation energy. Actually the effect is so pronounced that the highest-order reflections, which are readily seen at room temperature, are not resolved at the higher temperatures. Thus, for the purposes of data collection, the amplification of the detected pulses was increased so that the 512 channels of the analyzer covered 36·8 keV. Under these conditions, each channel spans an energy of about 71·0 eV and data were collected from the 333 to the 13,13,13 reflections only.

The procedure of collecting the data was as follows: once thermal equilibrium was established at each temperature, the spectrum was collected for a preset period of time. Although the pattern was readily discernible within a few minutes, a counting period of 40 minutes was used to insure good resolution of the higher-order reflections.

IV. Data reduction

A program develoed by Larson & Repace (1973) for analyses of spectral data collected with a solid-state detector was used to evaluate both the peak positions and the integrated intensities. This routine applies a linear background correction to each peak and uses a modified method of Zimmerman (1961) to determine the area under the peaks.

The measured intensities of the 777 reflection excited with Mo $K\alpha$ radiation were processed in the usual manner (*cf.* Skelton *et al.*, 1974). A correction was applied for the thermal diffuse scattering (TDS) contribution to the measured intensity with the procedure of Skelton & Katz (1968*b*); the values of the elastic stiffnesses required in this calculation were estimated from the phonon dispersion curve measurements of Smith & Gläser (1972). The TDS correction and more importantly its temperature dependence are found to be rather modest in this instance, amounting to only 1% at 296K and increasing to 2% at 600K. The corrected intensities are plotted as a function of temperature in Fig. 3 (triangles). If the TDS correction were ignored, the values of the intensity would still lie inside the triangular symbol, even at the highest temperatures. Because of the small effect of the TDS contribution in this case, as compared with the statistical fluctuation in the intensities themselves, it has been neglected in the subsequent analysis of the polychromatic data.

Consideration was also given to the Nb fluorescence radiation excited in the sample. The Nb $K\alpha$ radiation (16·58 keV) was observed between the 666 peak at 15·86 keV and the Mo $K\alpha$ radiation at 17·44 keV; however the Nb $K\beta$ line (18·62 keV) is included in the 777 Bragg reflection at 18·67 keV. Based on the measured intensity of the Nb $K\alpha$ peak and the $K\alpha/K\beta$ intensity ratio, the Nb $K\beta$ contribution to the measured 777 peak in this instance is estimated to be 0·11% at 296K and less than 0·15% at 520K. In consideration of the statistical scatter in the intensities, this correction was not believed to be significant.

The intensities of the 555, 777 and 10,10,10 reflections as evaluated at 13·27, 18·69 and 26·76 keV, respectively, are also plotted in Fig. 3 (solid circles). As noted above, the resolution of the higher-order lines tends to degrade, especially at elevated temperatures. This degradation is reflected through the increased scatter seen in the 10,10,10 data. It is further noted that the scatter in the intensity of the 777 peak is comparable for both the Mo $K\alpha$ and the polychromatic radiation measurements.

The polychromatic data have been analyzed by considering the room-temperature (296K) intensity as $\varrho'(T_0)$ and evaluating the intensity ratio for each of the elevated temperature measurements. The temperature dependence of this ratio was determined for each of ten *hhh* reflections ($h=3,4,\ldots,12$); this represents the left-hand side of equation (5). The right-hand side was evaluated in the following manner: since the position of the detector was invariant throughout the experiment, the $P(\theta)$ term and $P(\theta_0)$ term can be cancelled in equation (5). As will be shown below, the thermal expansivity of NbC is small and consequently the shift in E is also small, *viz.* about 40 eV over the temperature range of measurement. Recalling that this is less than the energy resolution of the detection system, it is reasonable to assume that $\Omega(E)\approx\Omega(E_0)$ in this case. It is noted however, that if this approximation were not applied, rather than attempt to evaluate

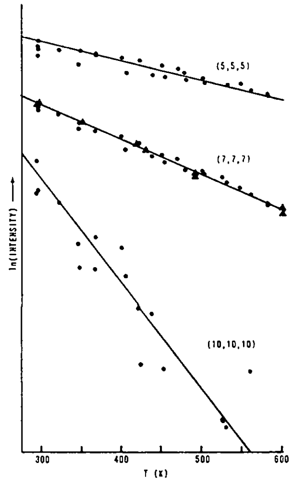

Fig. 3. Plot of the temperature dependence of the background-corrected intensities of the 555, 777 and 10,10,10 reflections recorded at 13·27, 18·69 and 26·76 keV, respectively (●) and of the 777 reflection recorded *via* conventional techniques at 17·443 keV (= Mo $K\alpha$) (▲). The solid lines through the data represent first-order least-squares curve fits.

$\Omega(E)$ for each reflection, it would be simpler to reset 2θ at each temperature in such a way as to keep E constant for each reflection. The $P(\theta)$ function is known and $P(\theta)/P(\theta_0)$ could be readily computed.

Based on the foregoing, equation (5) is reduced to the following form

$$\frac{\varrho'(T)}{\varrho'(T_0)} = \left[\frac{|f_{\mathrm{Nb}}\exp[-x\langle u^2_{\mathrm{Nb}}(T)\rangle]+\delta_{hkl}f_{\mathrm{C}}\exp[-x\langle u^2_{\mathrm{C}}(T)\rangle]|^2}{|f_{\mathrm{Nb}}\exp[-x\langle u^2_{\mathrm{Nb}}(T_0)\rangle]+\delta_{hkl}f_{\mathrm{C}}\exp[-x\langle u\ (T_0)\rangle]|^2}\right]. \tag{6}$$

The values of the atomic scattering factors were based on the calculations of Cromer & Waber (1965) for Nb and of Doyle & Turner (1968) for C; a dispersion correction was applied, based on the work of Cromer (1965). Values of $\langle u^2_{\mathrm{Nb}}(T_0)\rangle$ and $\langle u^2_{\mathrm{C}}(T_0)\rangle$ used in the analysis were 0·00750 ± 0·00060 Å^2 and 0·01071 ± 0·00124 Å^2 respectively; these values were based on independent room-temperature measurements made from the same sample (Feldman & Skelton, 1974). The remaining two unknowns in equation (6), $\langle u^2_{\mathrm{Nb}}(T)\rangle$ and $\langle u^2_{\mathrm{C}}(T)\rangle$, were found in the following manner: the measured temperature dependence of the intensity ratio of each of the recorded *hhh* reflections was least-squares fitted to a polynomial in T. It was found that the data could be adequately represented by a first-order polynominal, although higher-order terms were considered. Then for each value of T, equation (6) could be evaluated for the ten reflections, and finally a least-squares analysis was performed to find the values of $\langle u^2_{\mathrm{Nb}}(T)\rangle$ and $\langle u^2_{\mathrm{C}}(T)\rangle$ which best represented all the peaks recorded at the temperature T.

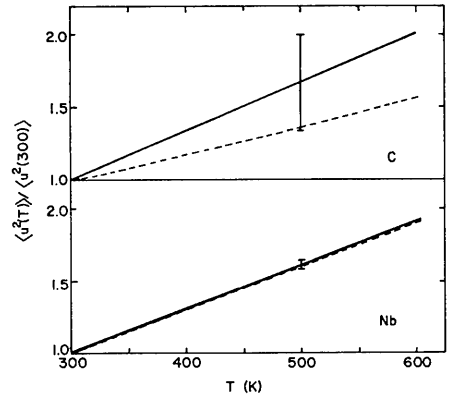

Fig. 4. Plot of the measured temperature dependence of the ratio of the mean-square atomic displacements, $\langle u^2(T)\rangle/\langle u^2(T_0)\rangle$ for the Nb and C atoms in NbC$_{0.98}$ (solid curve) and the published, computed values, (dashed curve).

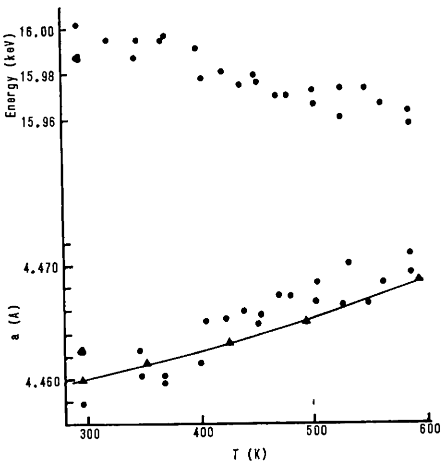

Fig. 5. Temperature dependence of the energy of the 777 peak recorded at a fixed 2θ angle (upper curve); the same data are expressed in terms of the unit-cell parameter in the lower curve (●). The triangles in the lower curve represent the change in the unit-cell parameter as determined from the shift in the 2θ position of the 777 peak at 17·478 keV (= Mo $K\alpha_1$). The solid curve represents a second-order least-squares curve fit to the triangle points.

Results and discussion

The values of $\langle u^2_{\mathrm{Nb}}(T)\rangle$ and $\langle u^2_{\mathrm{C}}(T)\rangle$ obtained from the energy-dispersive data vary linearly, within experimental uncertainty, over the temperature range 296 to 600K. The values of $\langle u^2_{\mathrm{Nb}}(T)\rangle$ increase from the previously determined value of $(7{\cdot}50 \pm 0{\cdot}60)\times 10^{-19}$ cm^2 at 296K to $(14{\cdot}42 \pm 0{\cdot}90)\times 10^{-19}$ cm^2 at 600K, while those for $\langle u^2_{\mathrm{C}}(T)\rangle$ increase from $(10{\cdot}71 \pm 1{\cdot}24)\times 10^{-19}$ cm^2 to $(21{\cdot}5 \pm 7{\cdot}1)\times 10^{-19}$ cm^2 over the same thermal range. The experimental uncertainties at 296K are based only on the previously reported room-temperature data (Feldman & Skelton, 1974); the error estimates at 600K are based on both the uncertainties in the reference values, plus those associated with the spectroscopic data, as computed from the least-squares analysis. Clearly the uncertainty in $\langle u^2_{\mathrm{C}}(T)\rangle$ is much larger than that in $\langle u^2_{\mathrm{Nb}}(T)\rangle$; the principal reason for this difference is believed to be due to the large difference in the atomic scattering factors for the Nb and C atoms, *e.g.* for the forward-scattered radiation, $(f_{\mathrm{C}}/f_{\mathrm{Nb}})^2 = 0{\cdot}017$.

These results may be compared with the recent force-model calculations of the MSD by Feldman & Skelton (1974), which are based on the double-shell model of Weber (1973). For purposes of comparing the measured and calculated temperature dependences, the ratios of the MSD are plotted in Fig. 4. Clearly, the agreement between theory and experiment is excellent for the Nb atom; but not too meaningful for the C atom owing to the experimental uncertainty.

As previously discussed, since the scattering geometry is held constant in this case, there is a small decrease in the energy of each peak with increasing temperature due to thermal expansion. This effect is represented graphically in Fig. 5: in the upper half of the figure the energy of the 777 peak is plotted *versus* temperature; this same information is shown in the lower part of Fig. 5 in terms of the unit-cell parameters (circles). For comparison, the temperature dependence of the unit-cell parameters, as determined from the 2θ shift in the Mo $K\alpha_1$ 777 peak, is also shown in Fig. 5 (triangles). Although the thermal expansivity could be determined from the energy shift, clearly the experimental uncertainty associated with the 2θ measurements is significantly smaller. This is reasonable since the energy resolution of the solid-state detection system is only 175 ± 6 eV, whereas the Mo $K\alpha_1$–$K\alpha_2$ doublet, which is readily resolved in 2θ at this angle, spans an energy gap of 105 eV. The fact that the single-crystal unit-cell parameters determined from angular dispersion data are more precise than those based on the energy dispersion is consistent with what has been previously concluded by others on the basis of polycrystalline measurements.

The thermal expansivity of $NbC_{0\cdot98}$ evaluated from the Mo $K\alpha_1$ data in Fig. 5 is about $6\cdot5 \times 10^{-6}$ K^{-1} at 600 K; this compares reasonably well with a value of $6\cdot3 \times 10^{-6}$ K^{-1}, computed from the data of Brenton, Saunders & Kempter (1969) for $NbC_{0\cdot969}$ and a value of $6\cdot90 \times 10^{-6}$ K^{-1} reported for $NbC_{0\cdot99}$ by Samsonov & Naumenko (1970).

Conclusions

It has been demonstrated that X-ray energy-dispersive diffraction data can be used to evaluate the temperature dependence of Debye–Waller factors. The procedure offers a number of improvements over the more conventional techniques, *viz.* speed, reduced geometrical requirements and measurement of higher-order reflections which might not otherwise be observable. Although absolute intensity measurements might require involved data processing, it is clear that many of those difficulties can be avoided by considering only relative changes in the intensity. The measured temperature dependences of $\langle u^2_{\rm Nb}(T)\rangle$ and $\langle u^2_{\rm C}(T)\rangle$ are both in agreement with recent lattice-dynamical force-model predictions over the thermal range of interest. The spectroscopic diffraction data have also been analyzed in terms of the thermal expansivity; a comparison with standard angular-dispersive expansion measurements based on the 777 $K\alpha_1$ peak shows the conventional method to be superior and to be in agreement with published expansivity measurements on NbC.

The author is grateful to Dr J. L. Feldman for many helpful discussions and to Dr H. G. Smith for providing the single crystal used in this study.

References

Albritton, L. M. & Margrave, J. L. (1972). *High Temp. High Press.* **4**, 13–19.

Blackman, M. (1956). *Acta Cryst.* **9**, 734–737.

Brenton, R. F., Saunders, C. R. & Kempter, C. P. (1969). *J. Less-Common Met.* **19**, 273–278.

Buras, B., Olsen, J. S., Gerward, L., Selsmark, B. & Anderson, A. L. (1975). *Acta Cryst.* A**31**, 327–333.

Cromer, D. T. (1965). *Acta Cryst.* **18**, 17–23.

Cromer, D. T. & Waber, J. T. (1965). *Acta Cryst.* **18**, 104–109.

Doyle, P. A. & Turner, P. S. (1968). *Acta Cryst.* A**24**, 390–397.

Feldman, J. L. & Skelton, E. F. (1974). *Phys. Lett.* **49**A, 127–128.

Freud, P. J. & LaMori, P. N. (1969). *Trans. Amer. Cryst. Assoc.* **5**, 155–162.

Giessen, B. C. & Gordon, G. E. (1968). *Science*, **159**, 973–975.

Larson, R. E. & Repace, J. L. (1973). NRL Memo Report 2658, NRL Computer Bull. 34, Naval Research Laboratory, Wash. D. C. 20375.

Samsonov, G. V. & Naumenko, V. Y. (1970). *Teplofiz. Vys. Temp.* **8**, 1093–1095.

Skelton, E. F. (1972). *Rep. NRL Progr.* pp. 31–33.

Skelton, E. F. & Katz, J. L. (1968*a*). *Phys. Rev.* **171**, 801–808.

Skelton, E. F. & Katz, J. L. (1968*b*). *Acta Cryst.* A**25**, 319–329.

Skelton, E. F., Lin, S. T. & Rothberg, G. M. (1974). *Acta Cryst.* A**30**, 39–43.

Skelton, E. F., Radoff, P. L., Bolsaitis, P. & Verbalis, A. (1972). *Phys. Rev.* **5**, 3008–3013.

Smith, H. G. & Gläser, W. (1972). In *Superconductivity in d- and f-Band Metals*, AIP Conf. Proc. No. 4, edited by D. H. Douglas, American Institute of Physics, New York.

Sparks, C. J. & Gedcke, D. A. (1972). *Advanc. X-Ray Anal.* **15**, 240–253.

Weber, W. (1973). *Phys. Rev.* B**8**, 5082–5092.

Zimmerman, W. (1961). *Rev. Sci. Instrum.* **32**, 263.